AIAA 80-1351R

Viscous Flowfield Solutions about a Finite Parabolic Body

Kenneth J. Weilmuenster*
NASA Langley Research Center, Hampton, Va.
and
Randolph A. Graves Jr.†
NASA Headquarters, Washington, D.C.

Abstract

A HYBRID computational technique that splits the flowfield into inviscid and viscous regions is used to investigate the complete flowfield about axisymmetric parabolic blunt bodies in a supersonic stream. The solutions are carried out on the CDC CYBER-203 computer which, with its extensive memory, allows for the use of a large number of finite-difference mesh points, allowing resolution of important flowfield features.

Contents

Analysis of the supersonic flow about blunt bodies has in the past been restricted by limited computational resources to flow over the forebody. This has led to some computational difficulties when the sonic line has moved outside of the computational domain; and, has left unresolved, the effect of base flow on the total drag of a blunt body. We have extended the hybrid computational technique described in Ref. 1 to investigate the complete flowfield about axisymmetric parabolic blunt bodies in a supersonic stream. The solutions are carried out on the CDC CYBER-203 vector computer, which with its extensive memory, allows for the use of a large number of finite-difference mesh points, allowing resolution of important flowfield features.

The physical coordinate system used in the description of the body and flowfield is the orthogonal parabolic system used in Ref. 2 and is formed by the intersection of curves belonging to two cofocal parabolas. The parametric equations for the Cartesian coordinates in this system are $x=\frac{1}{2}(\xi^2-\eta^2)$ and $y=\xi\eta$. As seen in Fig. 1, the axisymmetric body surface is formed by rotating the coordinate lines about the X axis. As described in Ref. 1, the flowfield is split into viscous and inviscid regions that are coupled along the line $\eta=\eta_c$, Fig. 1. The computational plane, in ξ and η, is rectangular with the physical boundaries corresponding to the simple rectangular boundaries of the computational plane. Coordinate stretching/compression is applied both in the forebody and afterbody regions to resolve important flowfield features.

Because the shock-fitting technique of Ref. 1 is used, the flow near the shock is considered to be inviscid and is governed by the conservative, compressible, time-dependent Euler equations. The remaining flowfield is governed by the full compressible, laminar, time-dependent Navier-Stokes equations in conservative form. The governing equations are cast in the form

$$\frac{\partial W}{\partial t}=-\frac{\partial F(W)}{\partial \xi}-\frac{\partial G(W)}{\partial \eta}+H(W)+S(W) \tag{1}$$

where the terms are the conserved quantities W, the convective terms F and G, the geometry terms H arising from a non-Cartesian coordinate system, and the viscous dissipation and heat conduction terms S, which are, of course, zero in the inviscid region. A complete listing of the governing equations may be found in Appendix A of Ref. 1. The metric coefficients for the orthogonal parabolic coordinate system given by the simple algebraic expression

$$h_\xi=(\xi^2+\eta^2)^{1/2} \qquad h_\eta=(\xi^2+\eta^2)^{1/2} \tag{2}$$

are substituted directly into the governing equations. These algebraic metric coefficients allow for the defining of the coinvariant velocities

$$u=h\mathfrak{U} \qquad V=h\mathfrak{V}$$

where

$$h=h_\xi=h_\eta \tag{3}$$

which eliminate errors caused by the differencing of nonlinear metric coefficients. The integration of the viscous equations is carried out by applying a modified version of the two-step Richtmeyer differencing algorithm described in Ref. 3, while the inviscid equations were integrated using the unsplit MacCormack technique.

Along the body surface, the usual no-slip boundary conditions, $u=0$ and $v=0$, are applied. The wall pressure is determined by setting the normal pressure gradient at the wall equal to zero. The wall density is then found from the equation of state by using the pressure and wall temperature which is held constant at some predetermined value. At the juncture of the fore- and afterbody surfaces, the wall pressure is double valued. For derivatives in the ξ direction that involve pressure, we use a wall pressure at the corner that has been determined from information along the line $\eta=\eta_0$ [see Fig. 1]. A similar procedure is used at the corner for derivatives in the η direction. Symmetry conditions are applied about the fore and aft stagnation lines, while the outflow boundary is set by second-order extrapolation of the conserved flow variables. The flowfield is always extended far enough downstream to insure supersonic flow at all points along the outflow boundary.

Generally, 6600 finite-difference mesh points are used with about 5600 of those being in the base region. This represents about one-half of the maximum that can currently be stored in the CDC CYBER-203 computer's central memory. In the numerical itegration of the governing equations, the local minimum time step is used[4] rather than the global minimum. This reduces the number of iterations (time steps) required to obtain a converged solution. Generally, the solutions required approximately 12,000-15,000 iterations to converge, which represents about 40 min of computation time on the CDC CYBER-203 computer.

Presented as Paper 80-1351 at the AIAA 13th Fluid and Plasma Dynamics Conference, Snowmass, Colo., June 14-16, 1980; submitted Sept. 18, 1980; synoptic received March 9, 1981. This paper is declared a work of the U.S. Government and therefore is in the public domain. Full paper available from AIAA Library, 555 W. 57th Street, New York, N.Y. 10019. Price: Microfiche, $3.00; hard copy, $7.00. **Remittance must accompany order.**

*Research Engineer, Aerothermodynamics Branch, Space Systems Division.

†Program Manager, Code RTF-6.

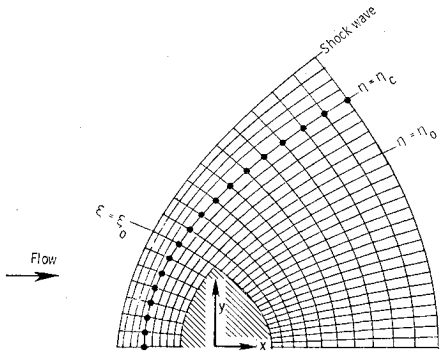

Fig. 1 Physical coordinate system.

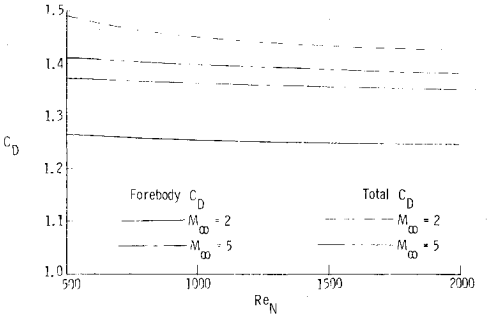

Fig. 3 Drag coefficient vs Reynolds number.

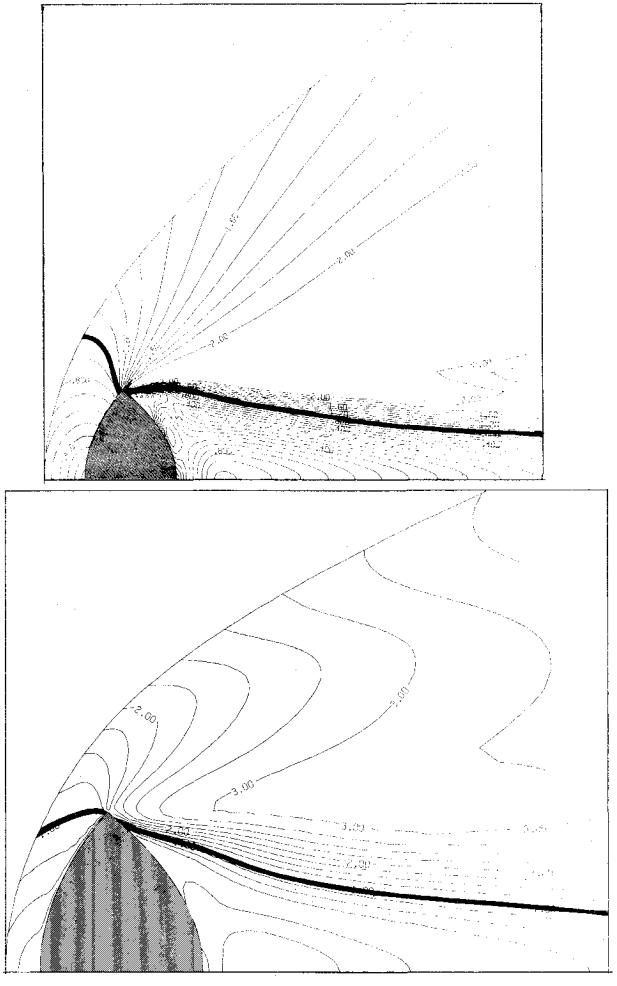

Fig. 2 Mach number contour plot; a) $M_\infty = 2$, $R_{eN} = 2000$; b) $M_\infty = 5$, $R_{eN} = 2000$.

In Figs. 2a and 2b, we show some results in the form of Mach number contour plots that encompass only a portion of the computed flowfield. The solid bounding curve on the left represents the discrete bow shock. For both the Mach 2 and 5 flows, the large expansion at the body corner and the base recirculation region are readily apparent. In both Figs. 2a and 2b, the sonic lines have been highlighted. The variations in the sonic-line shape are typical of the effects seen as the freestream Mach number was varied. Note, that at a Mach number of 2, a forebody-only analysis would be virtually impossible to carry out because the entire forebody region is subsonic. Figure 3 shows the effect of base flow on the total body drag which at low Mach numbers is significant. Furthermore, the results of this investigation have shown that the growth of the base recirculation region is a function of both Mach and Reynolds numbers, and that the growth rate is linear at higher Reynolds numbers for all Mach numbers. Further, at low Mach numbers, the base pressure varies significantly from the assumption of constant base pressure, while at high Mach numbers, this assumption appears to be quite good. Also, at the lower Mach numbers, the effects of base pressure and shear stress on total body drag are very pronounced, but have little effect on the drag at high Reynolds numbers.

References

[1] Weilmuenster, K. J. and Hamilton, H. H., "A Hybridized Method for Computing High Reynolds Number Hypersonic Flow about Blunt Bodies," NASA TP 1497, Oct. 1979.

[2] Peyret, R. and Viviand, H., "Calculation of the Flow of a Viscous Compressible Fluid Around an Obstacle of Parabolic Shape," NASA TT F-16558, 1975.

[3] Thommen, H. U., "Numerical Integration of the Navier-Stokes Equations," *Zeitschrift für Angewandte Mathematik und Physik*, Vol. 17, Fasc. 3, 1966, pp. 369-384.

[4] Kumar, A. and Graves, R. A. Jr., "Numerical Solution of the Viscous Hypersonic Flow Past Blunted Cones at Angle of Attack," AIAA Paper 77-172, Jan. 1977.